The aluminum HFI is almost isotropic, indicating largely s character although it is likely that some p contribution must be present but almost undetectable. The spin population at the aluminum, using an A_{iso} value of 1395 G, for an aluminum atom[14] is 0.024 and is remarkably close to the value of 0.028 for the methyl protons in methylallyl. Similar parallels exist for aluminum and hydrogens in vinyls[27,28] and allyls[29] with Al at the central carbon position.

Acknowledgment. J.A.H. and B.M. thank NATO for a research grant (No. 442/82) and B.M. thanks SERC for generous financial support.

(27) Kasai, P. H. *J. Am. Chem. Soc.* **1982**, *104*, 1165-1172.

(28) Howard, J. A.; Sutcliffe, R.; Tse, J. S.; Mile, B. *Organometallics* **1984**, *3*, 859-866.

(29) Howard, J. A.; Chenier, J. H. B.; Mile, B. *J. Phys. Chem.*, submitted for publication.

Angle-Selected ENDOR Spectroscopy. 1. Theoretical Interpretation of ENDOR Shifts from Randomly Orientated Transition-Metal Complexes

G. C. Hurst, T. A. Henderson, and R. W. Kreilick*

Contribution from the Department of Chemistry, University of Rochester, Rochester, New York 14627. *Received February 19, 1985*

Abstract: The NMR lines from ligand nuclei in paramagnetic transition-metal complexes are shifted because of the dipolar and Fermi contact interactions with the unpaired electron(s) of the metal ion. The dipolar interaction depends on the position of the nuclear spin with respect to the metal ion, and dipolar shifts can be analyzed to yield nuclear positions. This paper demonstrates how ESR spectra of randomly oriented molecules can be used to select molecular orientations. ENDOR spectra taken at orientations selected by ESR can then be used to determine nuclear positions and Fermi contact energies. A theoretical development of the equations for the shifts of ENDOR lines in randomly oriented solids is also given. This theory shows that the equations which have commonly been used to analyze ENDOR from these samples are incorrect and unable to account for many of the experimental features of the ENDOR spectra.

The electron spin of transition-metal ions interacts with ligand nuclear spins via dipolar and Fermi contact interactions, producing shifts in the NMR lines of the ligand nuclei.[1] The dipolar interaction depends on the relative position of the nuclear spin with respect to the metal atom, and the NMR spectra of solid samples can be analyzed to yield information about nuclear coordinates. NMR spectroscopy of solid paramagnetic samples has limited sensitivity so one can only examine relatively concentrated samples. Electron nuclear double resonance (ENDOR) is an alternative technique for obtaining nuclear resonance shifts of ligand nuclei in paramagnetic molecules. When nuclear and electron spin relaxation times are favorable, the technique yields a substantial sensitivity improvement and one can investigate magnetically dilute samples. ENDOR spectra are obtained by partially saturating an EPR transition and sweeping radio frequency radiation through nuclear resonance transitions.

EPR spectra of polycrystalline or amorphous samples reflect a "powder" average of all molecular orientations with respect to the magnetic field. If the $\bar{g}$ and hyperfine tensors are known, one can associate distinct sets of molecular orientations with a given resonant field value. This set of molecular orientations is thereby selected for nuclear resonance by the fixed field setting of the ENDOR experiment.[2-4] The result is an ENDOR spectrum that reflects the angular dependence of the hyperfine energies of ligand nuclei. Once this angular dependence is known, the geometric location of a ligand nucleus and spin density at that nucleus can be determined.

This idea has been applied in a variety of ENDOR studies of metal complexes to yield qualitative results. Much of the work done in powder ENDOR has not made full use of the angular selection which is provided by anisotropy in the EPR spectrum. The traditional equations used for powder ENDOR shifts have assumed that the electron and nuclear spins are quantized along the same axis and that the spin-only g value of the electron can be used to determine the dipolar field at the nucleus. These equations yield nearly correct answers in some limiting cases but are generally incorrect. We take a more complete approach, carefully considering the influence of angular selection on ENDOR powder spectra and making few simplifying assumptions in calculation of ligand nuclear resonant frequencies. With these methods, peak assignment is facilitated and accurate measurement of ligand nuclear coordinates in randomly oriented magnetically dilute paramagnetic samples is possible.

In this paper, we demonstrate more comprehensive techniques for using EPR spectra to select fixed molecular orientations for ENDOR investigations. ENDOR spectra have usually been taken only at the turning points of the EPR spectrum so that angular selection is limited to a few specific orientations. When frequency modulation of the swept rf radiation is employed, one is able to obtain ENDOR spectra throughout the EPR spectrum, thereby increasing the range of angular orientations which are selected. A theoretical development of the equations for ENDOR shifts in randomly oriented samples is also given, and results from this equation are compared with results from more commonly used equations for the analysis of ENDOR spectra. Techniques through which one can obtain information about molecular structure from angle-selected ENDOR experiments are illustrated for a typical copper complex. The equations are general, however, and can be used to determine local geometries of ligand nuclei near transition-metal ions in a variety of types of metal complexes. The

(1) Sandrezski, T.; Ondercin, D.; Kreilick, R. W. *J. Am. Chem. Soc.* **1979**, *101*, 2880. *J. Phys. Chem.* **1979**, *83*, 3388.
(2) Rist, G.; Hyde, J. *J. Chem. Phys.* **1968**, *49*, 2449.
(3) Rist, G.; Hyde, J. *J. Chem. Phys.* **1969**, *52*, 4532.
(4) Rist, G.; Hyde, J. *J. Chem. Phys.* **1969**, *52*, 4633.

0002-7863/85/1507-7294$01.50/0

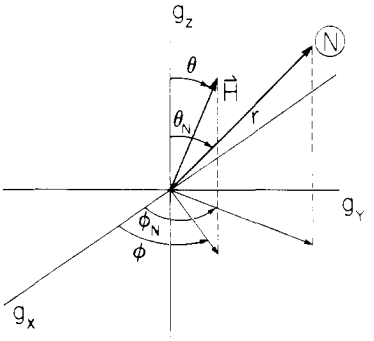

Figure 1. Coordinate system for EPR and ENDOR calculations showing applied field vector and nuclear position in the g axis system.

accompanying experimental paper confirms our theoretical predictions of ENDOR shifts and demonstrates how proton coordinates and contact energies are obtained from powder ENDOR spectra.

Angle Selection by EPR

The EPR spectra of magnetically dilute randomly oriented metal complexes with a single unpaired electron spin have been well-characterized in the literature.[5-7] The spectra of many of these complexes are dominated by g and metal nuclear hyperfine anisotropy. Quadrupole or ligand hyperfine energies, though sometimes resolved, do not contribute significantly to the overall angular dependence of the EPR powder pattern of most complexes. This type of spectrum is well described by the following Hamiltonian:

$$\mathcal{H}_e = \beta_e \hat{S}_e \cdot \bar{\bar{g}} \cdot \vec{H} + \hat{S}_e \cdot \bar{\bar{A}} \cdot \hat{I} \qquad (1)$$

In this equation β_e is the Bohr magneton, $\bar{\bar{g}}$ is the electronic g tensor, $\bar{\bar{A}}$ is the hyperfine tensor, $\vec{H}$ is the external field, and $\hat{S}_e$ and $\hat{I}$ are the electron and nuclear spin operators. Solution of this equation is achieved by a standard approach.[8] The electron Zeeman interaction is taken as the dominant energy term so that the coordinate system where the $\bar{\bar{g}}$ tensor is diagonal is a convenient frame of reference. Although the applied field is stationary in the experimental arrangement, it is better thought of, when dealing with powders, as a vector that can assume an arbitrary orientation in the $\bar{\bar{g}}$ axis system. With this view, the Hamiltonian is rewritten

$$\mathcal{H}_e = \beta_e H_0 \sum_{i=1}^{3} \hat{S}_i g_i h_i + \hat{S}_e \cdot \bar{\bar{A}} \cdot \hat{I} \qquad (2)$$

where $\vec{H} = [h_1, h_2, h_3]H_0$ and 1, 2, and 3 = x, y, and z.

The coordinate system used for these calculations and for ENDOR calculations is shown in Figure 1. The field components h_i can be written in this spherical polar coordinate system as:

$$h_1 = \cos\phi \sin\theta \quad h_2 = \sin\phi \sin\theta \quad h_3 = \cos\theta \qquad (3)$$

The final equation describing the resonant field position H_r in the EPR spectrum is

$$H_r = \frac{[h\nu - M_1 A(\theta,\phi)]}{\beta_e g(\theta,\phi)} \qquad (4)$$

where ν is the excitation frequency, h is Plancks constant, and M_1 is the metal nuclear spin quantum number. $A(\theta,\phi)$ and $g(\theta,\phi)$ are the field orientation dependent hyperfine and g values satisfying:

$$g(\theta,\phi) = [\sum_{i=1}^{3}(g_i h_i)^2]^{1/2}$$

$$A(\theta,\phi) = \frac{[\sum_{i=1}^{3}(\sum_{j=1}^{3} A_{ji} g_j h_j)^2]^{1/2}}{g(\theta,\phi)} \qquad (5)$$

(5) Sands, R. H. *Phys. Rev.* **1955**, *99*, 1222.
(6) Malmstrom, T.; Vanngard, T. *J. Mol. Biol.* **1960**, *2*, 118.
(7) Roberts, E. W.; Kosky, W. S. *J. Am. Chem. Soc.* **1960**, *82*, 3006.
(8) Abragam, A.; Bleany, B. "Electron Paramagnetic Resonance of Transition Metal Ions"; Clarendon Press: Oxford, 1970.

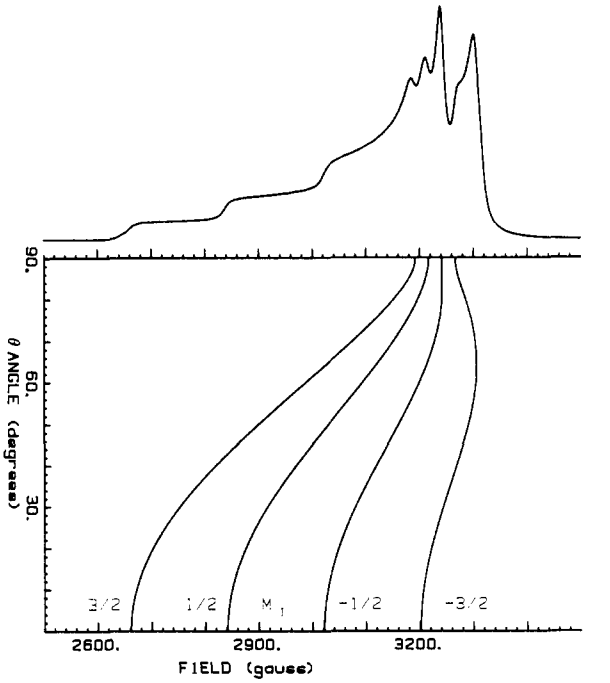

Figure 2. Selected orientations, specified as θ, shown as a function of applied field magnitude. Absorption profile above simulated with $g_x, g_y = 2.05$, $g_z = 2.259$, $A_x, A_y = 75$ MHz, and $A_z = 570$ MHz. Microwave frequency 9.27 GHz.

The equation shows that for each orientation of molecules with respect to the applied field, there is a field magnitude at which resonance occurs. For the purposes of ENDOR, however, one wishes to carry out the inverse calculation to determine which molecular angles are selected at a given resonant field position in the EPR spectrum. Each field value at resonance involves a specific set of molecular orientations which can participate in the ENDOR process. When the g and metal hyperfine tensors are axial and coincident, the selected orientations are particularly simple and the relationship between θ and the parameters in eq 5 may be expressed as a polynomial in $g(\theta,\phi)$

$$\left(\frac{\beta_e H_r}{hM_1}\right)^2 X^4 - \left(\frac{2\nu\beta_e H_r}{hM_1^2}\right) X^3 + \left[\left(\frac{\nu}{M_1}\right)^2 - \left(\frac{A_x^2 g_x^2 - A_z^2 g_z^2}{g_x^2 - g_z^2}\right)\right] X^2 + \left[A_z^2 g_z^2 - \left(\frac{A_x^2 g_x^2 - A_z^2 g_z^2}{g_x^2 - g_z^2}\right) g_z^2\right] = 0$$

with

$$\theta = \sin^{-1}\left[\frac{X^2 - g_z^2}{g_x^2 - g_z^2}\right]^{1/2} \qquad X = g(\theta,\phi) \qquad (6)$$

whose roots give θ at any given field value. The energy levels of rhombic systems[13,14] or systems with noncoincident $\bar{\bar{g}}$ and $\bar{\bar{A}}$ axes depend on both θ and ϕ, and the relationship between resonant field position and angles can be determined iteratively with a

(9) Neiman, D.; Kivelson, J. *J. Chem. Phys.* **1961**, *35*, 156.
(10) Orchinnikov, I. V.; Konstantinov, V. N. *J. Magn. Reson.* **1978**, *32*, 179.
(11) Schweiger, A.; Wolf, R.; Gunthard, H.; Ammeter, J. H. *Deiss Chem. Phys. Lett.* **1980**, *71*, 117.
(12) van Camp, H. L.; Scholes, C. P.; Mulks, W. S.; Caughey, J. *J. Am. Chem. Soc.* **1977**, *99*, 8283.
(13) Kneubuhl, F. K. *J. Chem. Phys.* **1960**, *33*, 1074.
(14) Griffith, J. S. "Theory of Transition Metal Ions"; Cambridge University Press: New York, 1971; Chapter 12.

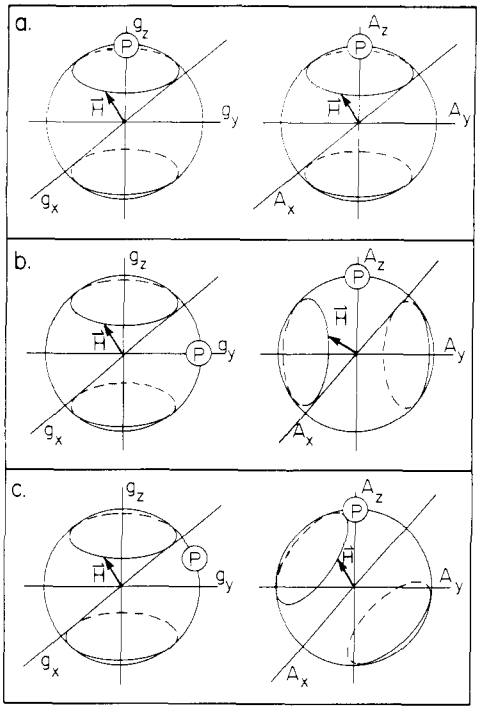

Figure 3. Surface of the spheres representing the isotropic distribution of molecular orientations present in a randomly oriented sample. The first column shows the set of selected orientations in the g axis system, along with a different proton position for each case a, b, and c. The second column shows the same set of field orientation as they appear within the principal hyperfine axis system. The paths on the spheres of column 2 indicate the frequencies present in the ENDOR spectrum.

computer. Figure 2 shows a plot of the θ selected at each value of the resonant field for an axially symmetric copper complex as well as the EPR spectrum of the complex. This figure illustrates how a given field magnetiude in the EPR spectrum selects groups of molecules with specific molecular orientations with respect to the applied field direction.

Figure 2 shows that up to four values of θ may be selected at higher fields where all four metal nuclear spin manifolds contribute to the EPR spectrum. In the lower field region of the spectrum where only $M_{+3/2}$ contributes to the spectrum, one can cleanly select single θ values ranging from about 0° to 40°. One can also select unique angles in the higher field part of the EPR spectrum where only the $M_{-3/2}$ level contributes to the spectrum. The dependence of the resonant field position on θ for this Cu energy level may be complicated when the hyperfine anisotropy is large compared to the g anisotropy. In this case, one will observe EPR "foldover"[9,10] ($M_{-3/2}$ level in Figure 2) where two values of θ are selected at a given field value.

Characteristics of ENDOR Spectra at Selected Molecular Orientations

The nuclear resonant frequencies of ENDOR spectra depend on the relative orientation of molecules with respect to the applied field. The ENDOR spectra for powders are taken at constant magnetic field where a unique set of field directions in the $\bar{\bar{g}}$ axis system is selected. The nuclear absorption frequencies present at any field value, therefore, are only those that are consistent with the field selected orientations. If the magnetic field is set to the low-field turning point in the EPR spectrum, one may in principle select a single orientation which would result in a "single-crystal" ENDOR spectrum.[5,11,12] At fields other than the low-field turning point, one selects orientations at a fixed θ but a range of values of ϕ. In these cases, a two-dimensional powder average is observed in the ENDOR spectrum. For molecules with axial symmetry and coincident $\bar{\bar{g}}$ and $\bar{\bar{A}}$ axes, the selected orientations can always be thought of as circles inscribed on the surface of a unit sphere coaxial with the g_z axis (Figure 3).

The ligand nuclear hyperfine tensor can have any symmetry or orientation. In the most general case, the tensor is fully

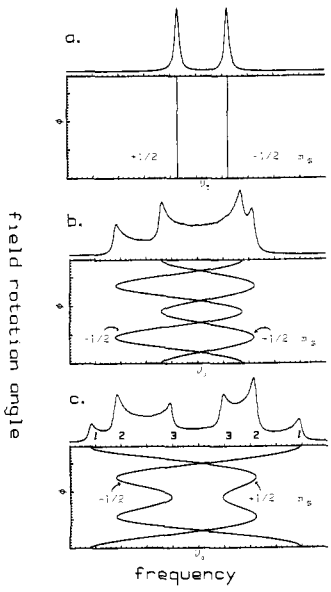

Figure 4. Simulated ENDOR powder patterns for a proton–metal distance of 2.5 Å and angular position as shown in Figure 3. The graphs show the dependence of ENDOR absorption frequency (in MHz) for a full rotation of ϕ (Figure 1) from 0° to 360°.

asymmetric and it is impossible to find a coordinate system where the hyperfine energy is diagonal. When the g anisotropy is small compared to the average g value, however, the tensor is only slightly asymmetric and the association of a unique coordinate system with a nucleus becomes a useful concept. Under these conditions, the maximum hyperfine energy occurs for a field pointed along the metal–nucleus vector (A_z axis) and the minimum when the field is near the A_x,A_y plane. The molecular orientations represented by the inscribed circles in the first column of Figure 3 ($\bar{\bar{g}}$ axis system), when transformed to the hyperfine coordinate system (second column of Figure 3), give the distribution of ENDOR frequencies.

Examples of the manner in which ENDOR spectra vary in a copper complex are illustrated in Figure 3. For complexes of this kind, the proton Zeeman energy is usually larger than the hyperfine splitting. When the proton is located along the g_z axis (Figure 3a), molecules selected at constant field all have the same pair of ENDOR frequencies ($m_s = \pm 1/2$). The ENDOR powder pattern, therefore, has two peaks at any value of θ. At other values of θ, the set of orientations produces a range of frequencies, but intensity builds at the extremes due to a slower change of frequency with orientation in that region. This phenomenon is equivalent to the "divergences" used by other authors[15,16] and is the origin of peaks in the powder pattern. When the proton is located in the g_x,g_y plane (Figure 3b), a four peak ENDOR spectrum is observed at any value of θ except $\theta = 0$, for which a single orientation is selected. In this instance, the ENDOR frequencies are reproduced identically in each of the four quadrants of the inscribed paths of Figure 3b. At other orientations of the ligand hyperfine tensor, this symmetry is destroyed. If the proton assumes coordinates intermediate to g_z and the g_x,g_y plane, a six peak ENDOR pattern is possible, three for each value of m_s (Figures 3c and 4c). This occurs because the selected frequency distribution is not symmetric for a reflection through the A_x,A_y plane as in the previous example. One pair of peaks arises from the absolute minimum in hyperfine energy that occurs in the A_x,A_y plane. The other two pairs are of different frequency in this example because of the skewed placement of the selected orientation curve in the hyperfine coordinate system.

Practical applications of these concepts to the extraction of nuclear geometries depend on being able to associate specific

(15) Lee, S. J. *J. Magn. Reson.* **1982**, *49*, 312.
(16) Hoffman, B. M.; Martinsen, J.; Venters, R. A. *J. Magn. Reson.* **1984**, *59*, 110.

applied field vectors with observed ENDOR peaks. Each of the diagrams in Figure 3 is constructed with a constant value of θ for the applied field in the $\bar{\bar{g}}$ axis system. Variation of the ENDOR frequencies in this context comes from the freedom in the angle ϕ to traverse values from 0° to 360°. ENDOR peaks, however, occur only at those values of ϕ where the frequency changes slowly with increments of ϕ. Two general conditions can produce powder pattern peaks. One occurs because the selected orientations pass through an absolute extreme in the hyperfine values as illustrated in peak 2 of Figure 4c. The other condition occurs when extremes of selected angles provide intensity accumulation as in peaks 1 and 3 of Figure 4c. For molecules with low symmetry, one may observe ENDOR peaks at an arbitrary collection of field orientations, but for some proton positions, the data may be equivalent to single-crystal rotations as will be shown in the accompanying experimental paper.

This discussion yields a qualitative picture of the basic features of an ENDOR powder pattern but does not allow quantitative predictions of the characteristics of these spectra. The next section of this paper develops the equations which give ENDOR transition frequencies as a function of the applied field vector and the magnetic tensors and relates nuclear coordinates to ligand nuclear hyperfine tensors.

ENDOR Transition Frequencies

Much of the work done on ligand ENDOR of powders or glasses has used the formula

$$\nu_{\pm} = |\nu_0 \pm A_N/2| \tag{7}$$

to calculate ENDOR transition frequencies (ν_0 = nuclear Larmor frequency, A_N = ligand nuclear hyperfine coupling). Other more complete theories have been applied in single-crystal ENDOR studies.[17-19] We have used the concepts developed for single-crystal analysis to derive a general theory for ENDOR transitions of randomly oriented samples. This development shows that the traditional formula (eq 7) is correct or nearly correct in special circumstances but is incomplete for a general analysis of ENDOR powder spectra. In a companion paper, we show that these theoretical predictions are observed experimentally.

Since an ENDOR spectrum is primarily a nuclear resonance spectrum, one must determine the total field at any given nucleus to calculate the transition frequency. Equation 8 is the Hamiltonian used to describe the spin $^1/_2$ ligand nuclear energies in an electron spin $^1/_2$ metal complex. If the coordinate system where

$$\mathcal{H}_N = \hat{S}_e \cdot \bar{\bar{A}}_N \cdot \hat{I} - g_N\beta_N\vec{H}\cdot\hat{I} = \sum_{i=1}^{3}[(\hat{S}_e\cdot\bar{\bar{A}}_N)_i - (g_N\beta_N H_0 h_i)]\hat{I}_i \tag{8}$$

the electron $\bar{\bar{g}}$ tensor is diagonal is used as a frame of reference, the nuclear spin, $\hat{I}$, will have three components $\hat{I}_1$, $\hat{I}_2$, and $\hat{I}_3$ where 1, 2, and 3 are the x, y, and z axes, respectively. In another coordinate system, the mathematical description of the nuclear spin energy levels is a scalar expression.

$$\mathcal{H}_N = K(m_s)\hat{I}_z' = K(m_s)M_I \tag{9}$$

The coefficients of $\hat{I}_1$, $\hat{I}_2$, and $\hat{I}_3$ in eq 8 are the projections of $K(m_s)\hat{I}_z'$ on the $\bar{\bar{g}}$ axes such that

$$K^2(m_s) = \sum_{i=1}^{3}[(\hat{S}_e\cdot\bar{\bar{A}}_N)_i - g_N\beta_N H_0 h_i]^2 \tag{10}$$

The value of $\hat{S}_e$ can be derived from the EPR data, and $\bar{\bar{A}}_N$ comes from the nuclear coordinates in the $\bar{\bar{g}}$ axis system. The applied field vector, $\vec{H} = [h_1,h_2,h_3]H_0$, along with expressions for $\hat{S}_e$ and $\bar{\bar{A}}_N$ yields the nuclear spin energy levels.

The electron spin vector, $\hat{S}_e$, is dependent on the $\bar{\bar{g}}$ tensor and the field direction and is not, for X-band EPR, always aligned parallel to the field. The expression for the electron spin is

$$\hat{S}_e = \frac{m_s}{g(\theta,\phi)}[g_1h_1, g_2h_2, g_3h_3] \tag{11}$$

The matrix $\bar{\bar{A}}_N$ is the sum of a dipolar term and an isotropic hyperfine interaction given by $\hat{S}_e\cdot\bar{\bar{A}}_N\cdot\hat{I}$. The isotropic Fermi contact term is small for most ligand nuclei, showing that most of the unpaired spin density is centered on the metal ion. Our derivation assumes that the electron is a point dipole located on the metal atom in the $\bar{\bar{g}}$ diagonal coordinate system. With this point dipole approximation, the field induced at any location in space by the electron dipole is given by

$$\vec{H}_d = \frac{\vec{\mu}_{e,m_s}}{r^3}\cdot(3\hat{r}\hat{r} - \bar{\bar{E}}) = \vec{\mu}_{e,m_s}\cdot\bar{\bar{A}}_d \tag{12}$$

where $\vec{\mu}_{e,m_s}$ is the electron magnetic moment, r is the distance from the electron to a nucleus, and $\hat{r}$ is a unit vector pointing in the direction of the electron–nuclear connecting vector. $\bar{\bar{E}}$ is the unit dyadic. When $\hat{r}$ is expressed in the $\bar{\bar{g}}$ diagonal reference frame and from

$$\vec{\mu}_{e,m_s} = -\beta_e\hat{S}_e\cdot\bar{\bar{g}} \tag{13}$$

the effective dipolar field at the nucleus is

$$\vec{H}_d = \frac{-\beta_e\hat{S}_e}{r^3}\cdot\begin{vmatrix} g_1(3r_1^2-1) & 3g_1r_1r_2 & 3g_1r_1r_3 \\ 3g_2r_1r_2 & g_2(3r_2^2-1) & 3g_2r_3r_2 \\ 3g_3r_1r_3 & 3g_3r_2r_3 & g_3(3r_3^2-1) \end{vmatrix} \tag{14}$$

with $r_1 = \cos\phi_N \sin\theta_N$, $r_2 = \sin\phi_N \sin\theta_N$, and $r_3 = \cos\theta_N$. The hyperfine energy expressed in eq 8, $\hat{S}_e\cdot\bar{\bar{A}}_N\cdot\hat{I}$, must be equal to the energy of a proton (or other spin $^1/_2$ nucleus) in the dipolar field $g_N\beta_N\vec{H}_d\cdot\hat{I}$. Therefore, with the isotropic term included, the explicit expression for the $\bar{\bar{A}}_N$ of eq 8 in frequency units is

$$A_{ij} = \frac{-\beta_e g_N\beta_N}{hr^3}g_i(3r_ir_j - \delta_{ij}) + A_{iso}\delta_{ij} \tag{15}$$

The nuclear spin energy levels are related to the hyperfine coupling, the moment of the electron, and the field direction by eq 8 and 9 and the allowed nuclear transitions occur for $\Delta M_I = \pm 1$. Substitution of (15) and (11) into (10), with conversion from energy to frequency units, yields a final expression for the frequency of ENDOR transitions

$$\nu(\vec{H},m_s) = \left[\sum_{i=1}^{3}\left[\frac{m_s}{g(\theta,\phi)}\left(\sum_{j=1}^{3}g_jh_jA_{ji}\right) - h_i\nu_0\right]^2\right]^{1/2} \tag{16}$$

$$\nu_0 = g_N\beta_N H_0/h$$

Equation 16 gives the resonant frequency of a nucleus of known coordinates as a function of field direction $[h_1,h_2,h_3]$ and magnitude H_0. This equation accounts for the electron and nuclear spins being quantized along different directions, the dipolar and applied fields having different directions but comparable magnitudes and the average electron magnetic moment being field vector dependent.

The equations for transition frequencies traditionally used in powder ENDOR studies (eq 7) are often used with the following expression for the hyperfine coupling to relate electron–nuclear separations and dipolar angles to ENDOR shifts.

$$A_N = \frac{g_N\beta_N g_e\beta_e}{r^3}(3\cos^2\theta - 1) + A_{iso} \tag{17}$$

These equations include the implicit assumptions that the electron and nucleus are quantized along the applied field direction and that the spin-only g value is adequate for calculation for the dipolar tensor. These assumptions are valid for nuclei that are far away from from the paramagnetic center but are not generally correct. Equation 7 predicts that nuclear resonances occur symmetrically about the free nuclear frequency and are independent of the electron g value. Equation 16 shows that the pairs of frequencies ($m_s \pm ^1/_2$) are not always symmetric about the nuclear Larmor frequency and do depend explicitly on the electron $\bar{\bar{g}}$ tensor. These

(17) Schweiger, A.; Graf, F.; Rist, G.; Gunthard, H. *J. Chem. Phys.* **1976**, *15*, 155.
(18) Hutchison, C.; McKay, D. B. *J. Chem. Phys.* **1977**, *66*, 3311.
(19) Iwasaki, M. *J. Magn. Reson.* **1974**, *16*, 417.

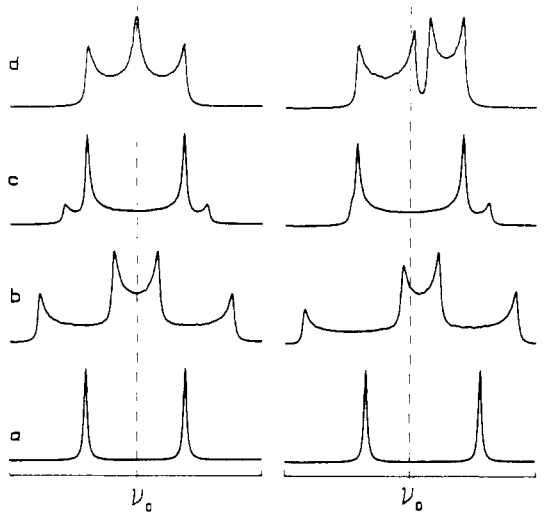

Figure 5. Comparison of simulations from eq 7 and 17 (right side) with results using eq 15 and 16 (left side) for a proton 2.5 Å from the metal center. The field direction parameter θ is 30° in each case. The angular proton position θ_N is (a) 0°, (b) 30°, (c) 60°, and (d) 90°.

effects are observable in experimental ENDOR spectra and facilitate the analysis and extraction of structural information from ENDOR powder data. Figure 5 compares spectra calculated by using the traditional formula (eq 7) with those calculated with eq 16 at a series of proton positions. The spectra calculated with the correct equation have different ENDOR transition frequencies than those found when one uses eq 7 and clearly show asymmetry in peak position with respect to the nuclear Larmor frequency. These differences may be observed both in the single-crystal and two-dimensional powder spectral regions.

The two-dimensional powder spectra calculated with eq 16 show that some of the peaks in the pattern may be shifted to higher frequencies while others remain symmetric about ν_0. These shifts are most readily explained by transforming eq 16 to the coordinate system where the pure dipolar interaction is diagonal ($\bar{A}_d$ of eq 12) and assuming that the g anisotropy is small enough that the electron spin is approximately collinear with the applied field. Equation 16 then takes the form

$$\nu(\vec{H},m_s) = \left[\sum_{i=1}^{3}\left(\frac{m_s}{g'(\theta,\phi)}g_i'h_i'A_{ii} - h_i'\nu_0\right)^2\right]^{1/2} \quad (18)$$

where h_i' are the field direction cosines expressed in the new axis system. If the applied field is oriented so that h_z' is unity, eq 18 becomes

$$\nu(\vec{H},m_s) = \left[\left(\frac{m_s g_3'}{g'(\theta,\phi)}A_{33} - h_i'\nu_0\right)^2\right]^{1/2} = |\nu_0 \pm A_{33}/2| \quad (19)$$

This equation shows that field orientations that correspond to a principal axis of the proton hyperfine tensor produce symmetric transition frequencies, while both m_s transitions are shifted to higher frequencies for other orientations.[20] Equation 19 can only be approximately true, however, because of the inherent asymmetry of the hyperfine tensor. In complexes where the g anisotropy is a small percentage of the average g value, the concept of a diagonal hyperfine tensor is useful for spectral interpretation. In systems with large g anisotropy, the electron spin $\hat{S}_e$ is no longer oriented parallel to the applied field and the hyperfine tensor is so distorted that diagonalization is impossible. In these cases, symmetric ENDOR peaks are guaranteed only when the applied field and the proton lie along a principal $\bar{\bar{g}}$ axis. When a proton is located along the g_z axis of copper, m_s pairs in the ENDOR spectrum are symmetric when the field points along g_z or is in the g_x,g_y plane, but at intermediate fields (and associated θ values as in Figure 2), the peaks are asymmetrically placed around ν_0 (Figure 4a). For other combinations of field direction and nuclear coordinates, some of the pairs are symmetric and others are asymmetric (Figure 4c). Observation of symmetric and asymmetric pairs, with comparison to the field selected angles, reveals the angular position of the nucleus. When the nucleus lies in the g_x,g_y plane (Figure 3b), symmetric peaks occur both when the field is along g_z and when it is in the g_x,g_y plane. These are the two observing fields that have most often been used in powder ENDOR investigations of planar complexes and explains why the inadequacy of the traditional formulas was not observed sooner.

(20) Schweiger, A. "Electron Nuclear Double Resonance of Transition Metal Complexes with Organic Ligands; Structure and Bonding"; Springer-Verlag: New York, 1982; Vol. 51, p 29.

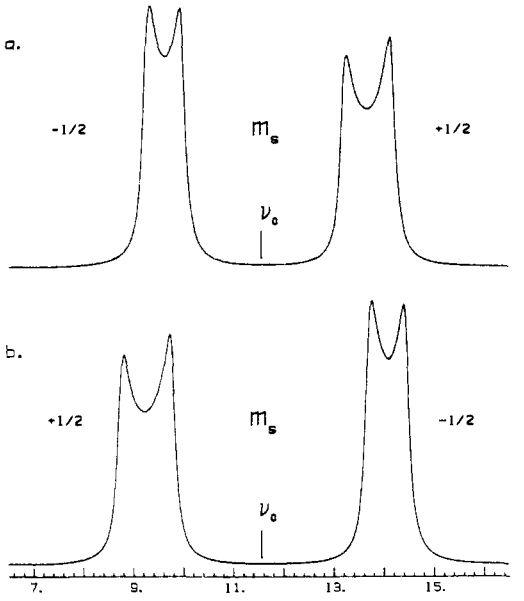

Figure 6. Asymmetry of ENDOR frequency pairs ($m_s = \pm^1/_2$) removing ambiguity in determination of the Fermi contact energy. Spectrum a was simulated with $A_{iso} = -9.0$ MHz, spectrum b with $A_{iso} = 0.6$ MHz. The proton is 3.1 Å from the paramagnetic center at an angle of 10° from the g_z axis. The θ value for the field is 20° in both cases. Simulations using eq 7 would be virtually indistinguishable.

In this context of relatively low g anisotropy, peak asymmetry can be a guide to the metal–nucleus distance. If the nucleus is far away from the metal, the dipolar interaction decreases to zero and only the contact term will remain. Since the isotropic contact interaction is diagonal in any coordinate system, peaks will be symmetric for distant protons. ENDOR pairs that are appreciably asymmetric, therefore, can be associated with protons that are close (less than 4 Å) to the metal ion.

The asymmetric nature of some transition frequency pairs also removes an ambiguity in the determination of the sign and magnitude of the isotropic coupling constant. The shift to higher frequency in asymmetric pairs is not equal in each electron spin manifold so that each m_s branch of the pattern traverses a somewhat different range of frequencies. The two branches arise from equal numbers of molecules but since one manifold covers a larger frequency range than the other, the density of the resonant transitions in the pattern of the larger frequency range is less than in the narrower pattern. The difference in resonant transition density translates into an observed intensity difference in the two m_s branches of the pattern. Figure 6 shows that two values of A_{iso} that give the same spectrum with eq 7 are uniquely determined with the theory of eq 16.

The electron $\bar{\bar{g}}$ matrix also figures prominently in the prediction of ENDOR transition frequencies. Anisotropy in g guarantees a rhombic ligand hyperfine tensor except when the proton is located along g_z. This anisotropy causes perturbations in the hyperfine splitting that depend on the orientation of the applied field. A proton located in the plane offers a good example of this. If the observing field is along g_z as in Figure 7a, the hyperfine splitting is appropriate for the effective g value in this direction. When $\theta = 90$ and the field is in the plane (Figure 7a), a different

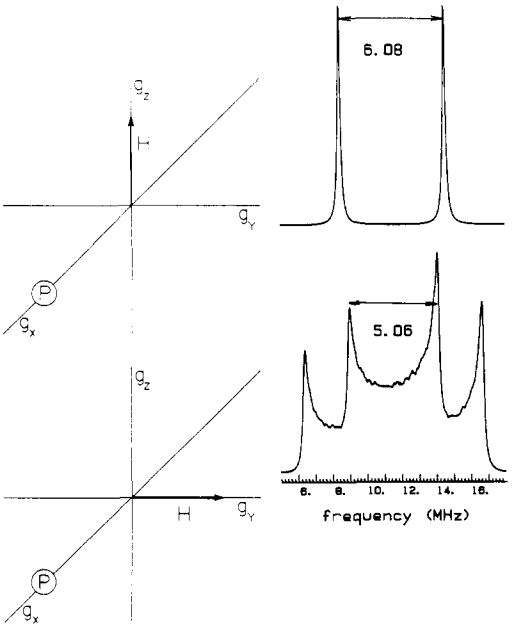

Figure 7. Simulations for a proton 2.5 Å from the metal center showing the effect of g anisotropy on ENDOR splitting. $g_y = 2.05$, $g_z = 2.4$.

splitting is observed for the peaks created when the field is along the g_y axis. Even though the field makes a perpendicular angle with the electron–proton vector in each case, the hyperfine energy is different due to anisotropy in the electron $\bar{g}$ tensor. This effect is observable in experimental ENDOR spectra from randomly oriented samples.

In order to determine nuclear geometries and spin densities from ENDOR spectra, one must be able to determine the correspondence between observed ENDOR peaks and the direction of the molecule in the applied field. The applied field magnitude, along with the EPR parameters, provides information about the field directions that may give rise to ENDOR peaks. Nuclear geometric parameters and field directions used in calculations of ENDOR peak positions with eq 16 must be able to reproduce experimental peak positions for spectra acquired at different field magnitudes. Asymmetry about the free nuclear frequency and dependence of ENDOR shifts on the effective g value help in the assignment of peaks to specific protons and field orientations. The method is illustrated in the accompanying experimental paper for a polycrystalline copper complex.

Conclusions

This paper has given the theoretical foundation for a comprehensive analysis of ENDOR powder spectra. We have shown that irradiation of any region of an EPR spectrum allows one to select a distinct group of molecular orientations for acquisition of ENDOR data. Interpretation of ENDOR peaks at one field magnitude must be consistent with interpretations at all other field values, placing stringent conditions on peak assignment and nuclear coordinates. Our derivation of a general equation for ENDOR transition frequencies shows that the equation which has commonly been used to analyze powder ENDOR spectra is incorrect. The correct equation predicts that some powder pattern peaks will occur asymmetrically about the free nuclear frequency and that ENDOR shifts depend on the effective electron g value.

Acknowledgment. This work was supported in part by National Institute of Health Grant GM22793 and by a graduate research fellowship from the Eastman Kodak Co.

Angle-Selected ENDOR Spectroscopy. 2. Determination of Proton Coordinates from a Polycrystalline Sample of Bis(2,4-pentanedionato)copper(II)

T. A. Henderson, G. C. Hurst, and R. W. Kreilick*

Contribution from the Department of Chemistry, University of Rochester, Rochester, New York 14627. *Received February 19, 1985*

Abstract: Angle-selected ENDOR experiments have been performed with polycrystalline samples of bis(2,4-pentanedionato)palladium(II) doped with Cu(II). These experiments allowed the position and Fermi contact energy for a nearby proton to be determined from a randomly oriented sample. The experiments also confirm theoretical predictions of the asymmetric arrangements of ENDOR peaks with respect to the nuclear Zeeman frequency, the g value dependence of ENDOR shifts, and the dependence of ENDOR peak intensities on the electron spin quantum number.

Anisotropy in the EPR spectra of noncrystalline metal complexes can be used to select specific molecular orientations with respect to the external magnetic field.[1] The EPR "powder" spectrum arises from randomly oriented molecules but when the field is fixed at a specific value, only molecules at certain orientations contribute to electron resonant absorption. When g anisotropy dominates the angular dependence of the EPR spectrum, it is convenient to describe the selected molecular orientations with reference to the principal $\bar{g}$ axis system.[2] Electron nuclear double resonance (ENDOR) spectroscopy involves setting the external magnetic field to a specific EPR transition and sweeping radio frequency radiation through nuclear transitions while monitoring the EPR absorption. The ENDOR shifts thus obtained reflect electron–nuclear dipolar and Fermi contact hyperfine interactions. If one makes use of the angular selection provided by the EPR field setting, one is able to analyze ENDOR shifts to determine the Fermi contact energy of ligand nuclei and their position with respect to the principal $\bar{g}$ axis system. Angle-selected ENDOR spectroscopy, therefore, provides a powerful technique for determination of ligand structures in polycrystalline or glassy samples.

The theoretical analysis used in most ENDOR studies of randomly oriented samples has involved some erroneous as-

(1) Hurst, G.; Henderson, T. A.; Kreilick, R. W. *J. Am. Chem. Soc.*, preceding paper in this issue

(2) Abragam A.; Bleany B. "Electron Paramagnetic Resonance of Transition Metal Ions"; Clarendon Press: Oxford, 1970.

0002-7863/85/1507-7299$01.50/0